Measurement of mechanical properties of pig bone: comparison between finite element model and experimental test

Cristian Andres Hernandez Salazar, O González-Estrada

RESEARCH REPORT-WORKING PAPER V.1

MEASUREMENT OF MECHANICAL PROPERTIES OF PIG BONE: COMPARISON BETWEEN FINITE ELEMENT MODEL AND EXPERIMENTAL TEST

Cristian A Hernández-Salazar
Octavio A González-Estrada

Bucaramanga-Santander-Colombia 2022

Research Group on Energy and Environment – GIEMA
School of Mechanical Engineering
Universidad Industrial de Santander

Measurement of mechanical properties of pig bone: comparison between finite element model and experimental test

Cristian A Hernandez_Salazar[1], O. González-Estrada [2]

[1] ingeniero Mecánico, cahss77@gmail.com, ORCID 0000-0002-9915-6384, Universidad Industrial de Santander, Bucaramanga, Colombia.
[2] PhD Ingeniería Mecánica, agonzale@saber.uis.edu.co, ORCID 0000-0002-2778-3389, Universidad Industrial de Santander, Bucaramanga, Colombia.

1. Introduction

The finite element model (FEM) of bones has become a great tool to predict the outcome of in vivo practices [1]. Its appearance in the orthopaedic field occurs in 1972 and since then, its use has been increasing in areas such as prosthesis design, to obtain structural data of bones and for evaluating tissue deterioration over time [2]. Recently, finite element models, in addition to describing and characterizing tissues, corroborate or discard hypotheses related to the intervening forces in a certain region of the body, or materials to be used in the prevention of tissue wear, and even the pressure exerted by inter-articular ligaments, faster and more efficient [3], [4], [5], [6].

The way in which finite element models have been made is by taking data from X-rays, computed tomography (CT), micro computed tomography (μCT), high-resolution peripheral computed tomography (HR-pQCT) and magnetic resonance imaging (MRI). From which a DICOM (Digital Imaging and Communications in Medicine) file is obtained that can be processed in different software to generate meshes of identical geometry to the study geometry [7]. With the development of technology in the quality of the machinery for taking images, progress has also been made in more specialized and detailed studies for the realization of finite element models (FEM). This is how models obtained from μCT and HR-pQCT have turned out to be more reliable, however, this quality is directly related to the amount of radiation that affects the tested specimen [8].

Obtaining a finite element model has another inconvenient, this is related to the handling of the mechanical properties of the material that is assigned to the mesh obtained. Some studies have erroneously used homogeneous isotropic properties to describe the properties of an organic material [9], this may be in response to faster and less complex data processing. However, the most recent studies point to the manipulation of properties of organic tissue by voxel [10]. This method consists of assigning independent mechanical properties to the scanned element according to its gray scale, this is represented with Hounsfield units (HU) which at the same time indicate the intensity of each pixel in the image [11]. HU units indicate a quantitative amount of radiological density and have been related to the Young's modulus of materials [12].

In this study, the segmentation of pig leg bones obtained from standard CT scanning is performed. Subsequently, the segmentation is digitally evaluated through the software ANSYS, specimens are tested by varying their geometries and in the same way the voxel technique is applied (taking into account the HU and grey scale assigned by the literature for the pig femur), as well as isotropic properties (trabecular and cortical tissue) of the material in order to establish the differences

between the two methods. The evaluation in ANSYS allows the researchers to determine the area of failure of each geometry as well as the maximum stress supported.

In addition to the above, in vivo experimentation is carried out, where compression tests determine the maximum stresses and deformations, which allows to find the resistance of the tested specimen. Finally, the experimental and digital data obtained in the FEM analysis are compared.

2. State of the Art

For this article there were reviewed more than 500 articles that were linked somehow to this study, some of them developing strategies for accurate digital processing of DICOM images, such as said by Moosmann *et al.* [13] in his study where they develop a method to acquire images from the tomograph. Others were interested in figuring out the forces and strength of some body parts such as some ligaments and tendons [4], [5]. Some others evaluated new methods and materials being tested by FE models, [3], [14].

Table 1. Search in Scopus. Shows five different Booleans that were used in this study to acquire information about what has been made worldwide. Information was obtained from Scopus database in order to find the majority of articles corresponding to what was searched for.

Table 1. Search in Scopus.

Boolean	Total results	Relevant results for this study
TITLE-ABS-KEY (bone AND segmentation AND mechanical AND properties)	117	9
TITLE-ABS-KEY (pork OR pig OR piglet AND bone AND segmentation AND mechanical AND properties)	5	0
TITLE-ABS-KEY (pork OR pig OR piglet AND bone AND mechanical AND properties)	342	10
TITLE-ABS-KEY (pork OR pig OR piglet AND bone AND segmentation)	42	1
Total	**506**	**20**

Relevant results were chosen in terms of similarity with this investigation, all of them that had to do with bones of pigs, acquiring images from tomography, and evaluation by FEM models having into account the grey scale method for assigning materials. Afterwards, the 506 articles were evaluated by co-occurrence with the software VOSviewer Fig. 1. Clusters created by VOSviewer.And Fig. 2. Cluster 1, 2, 3 and 4 respectively. Show all the links, connections as well as the time when they were the most used. It can be seen in Fig. 1. Clusters created by VOSviewe There were four clusters obtained, those, correspond to four areas linked to other words that were classified in the same area.

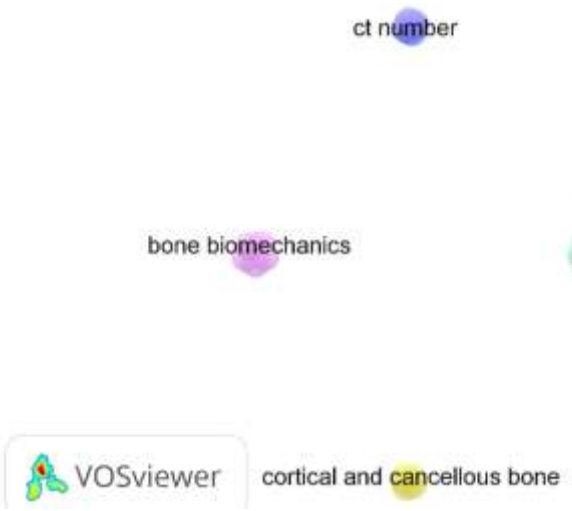

Fig. 1. Clusters created by VOSviewer.

Clusters shown in Fig. 2. Cluster 1, 2, 3 and 4 respectively.Are corresponding to each of the areas selected by VOSviewer. As it can be seen all the words have the same weight, it means same co-occurrence, but what differentiates all clusters is the quantity of links between words having the first one many more than the rest of them.

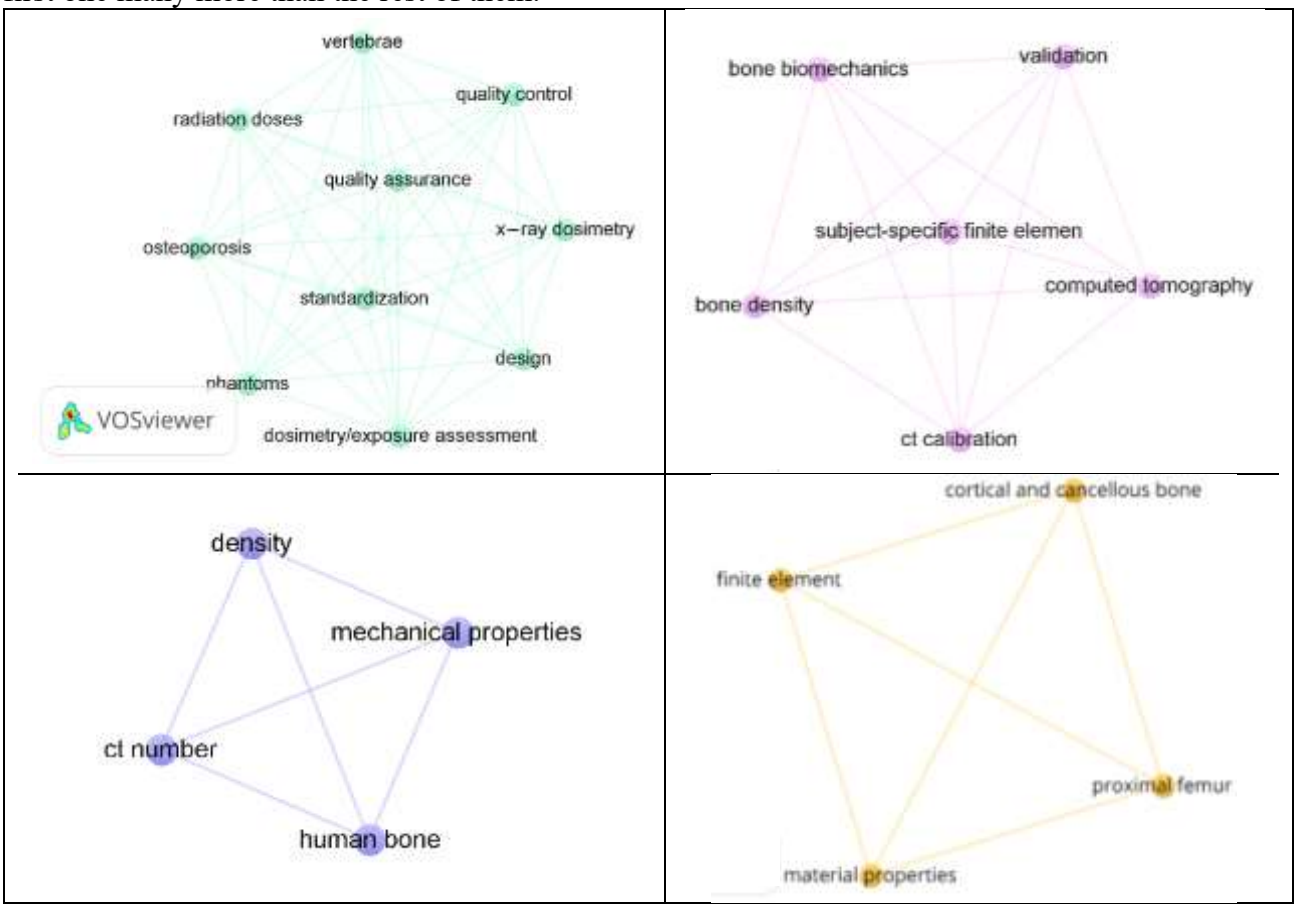

Fig. 2. Cluster 1, 2, 3 and 4 respectively.

The following figure (Fig. 3. Keywords throughout the years.), demonstrates how taking about FEM is been done since around 2010. As it can be seen by the distribution of the clusters, same as in Fig. 1. Clusters created by VOSviewer. Cluster 4 contains the words that have been most recently used. All of his keywords correspond directly to making FE models, so it reinforces the idea of making digital instead of in vivo evaluations to material properties.

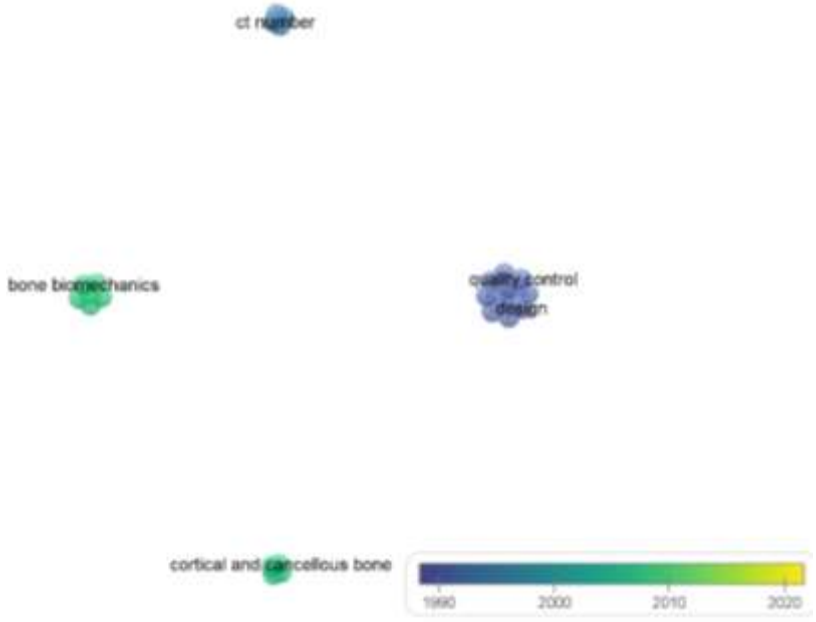

Fig. 3. Keywords throughout the years.

3. Materials and methods

The aim of this section is to assure that samples are treated as equal to determine precise differentiation from each specimen. The compressive tests were made with different geometries following other studies protocols. Afterwards, tests following the experiment were made digitally adding other variable, isotropic material vs orthotropic material. Finally all the obtained data was processed and compared.

3.1. Medical imaging and bone segmentation

A computerized axial tomography was performed at the Hospital Universitario de Santander where a fresh pig leg obtained from a butcher shop in the area was segmented. The specimen was transported taking into account a controlled temperature chain to ensure the good condition of the specimen. 832 slices were obtained which were saved as a DICOM file that was later processed in software. The pig's leg contained 5 bones, including part of the hip, the entire femur, the patella, and part of the fibula and tibia.

The DICOM file was processed in the free software 3D Slicer version 4.10.2, from which the five meshes corresponding to each of the bones found in the scanned pig leg were obtained. Subsequently, each one of the meshes was stored separately and the mesh corresponding to the

femur was edited to match its characteristics with the real bone to which the mechanical compression tests were applied. In Fig. 4. It can be seen the segmentation process carried out from the DICOM data.

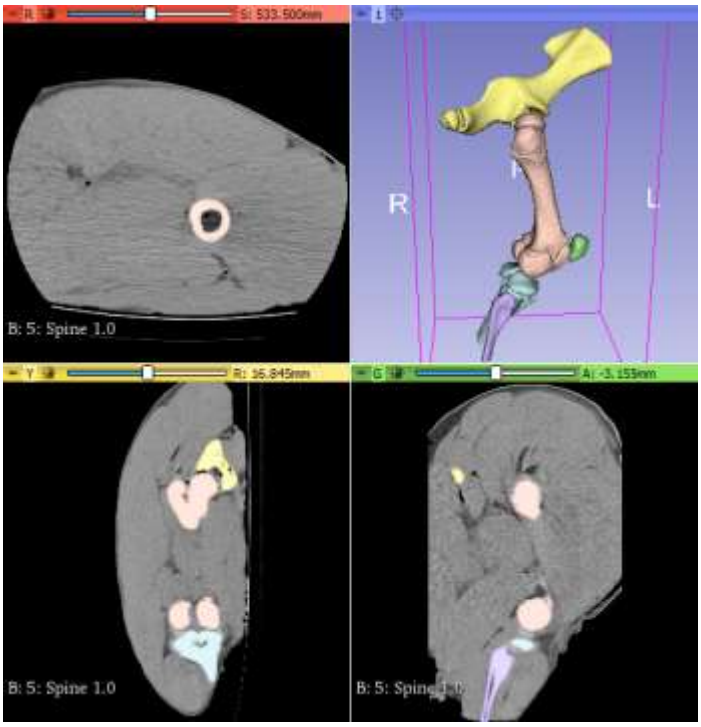

Fig. 4. Segmentation in 3D Slicer software.

3.2. Bone preparation and mechanical test

The muscle tissue was removed from the piece leaving the five parts of bone tissue, later a manual cleaning of the bone was carried out in order not to affect its mechanical properties. The bone was stored in a freezer, soaked in saline solution. Fig. 5. Bone cleaning. Shows the condition of the bones prior to storage.

Fig. 5. Bone cleaning.

Before the compressive testing each bone was warmed up by leaving them into room temperature 24 hours before. Then there were performed different cuts to each bone using a core drilling

machine and a handsaw from the industrial design laboratory at the Universidad Industrial de Santander.

The protocol for the compressive test was made following the ones made in [15] and [16] in where there were made cylinders of different radius and height from each bone in order to calculate the stress rate. this study had into account the recommendations made in [17] where they determine that small specimens produce errors.

The compressive test was conducted by MTS compressive machine. As well as in [16] samples were preloaded with a force of 50N at a 2mm/min velocity. Data were processed to determine Young modulus, yield and ultimate stress.

3.3. Finite Element Model

Static analysis was performed with the software ANSYS in where there was put each mesh corresponding to each specimen cut in the experiment with the same measurements. In ANSYS two analysis were made, the first one with an anisotropic material and the second one with an isotropic material.

Resolution of the mesh in element finite can be verified with table 1, where the resolution of the mesh is observed.

Table 1. Resolution of the mesh in element finite

Resolution	Nodos	Elements	Displacement mm	% error
2	11258	7623	0,544	2,472
3	13326	8396	0,557	0,395
4	26089	16896	0,559	-

Anisotropic Material Assignment
The process of assigning material for each element of the mesh was carried out using the free software Bonemat, where files corresponding to the tomographic images and the corresponding mesh were attached. This software assigns Young's modulus values based on the densitometric calibration of the CT. The values of the relationships were taken according to [18] where ESP calibration proposed by Kalender is used [19]. In Fig. 66. The differentiation by color of the different materials existing in the mesh is appreciated.

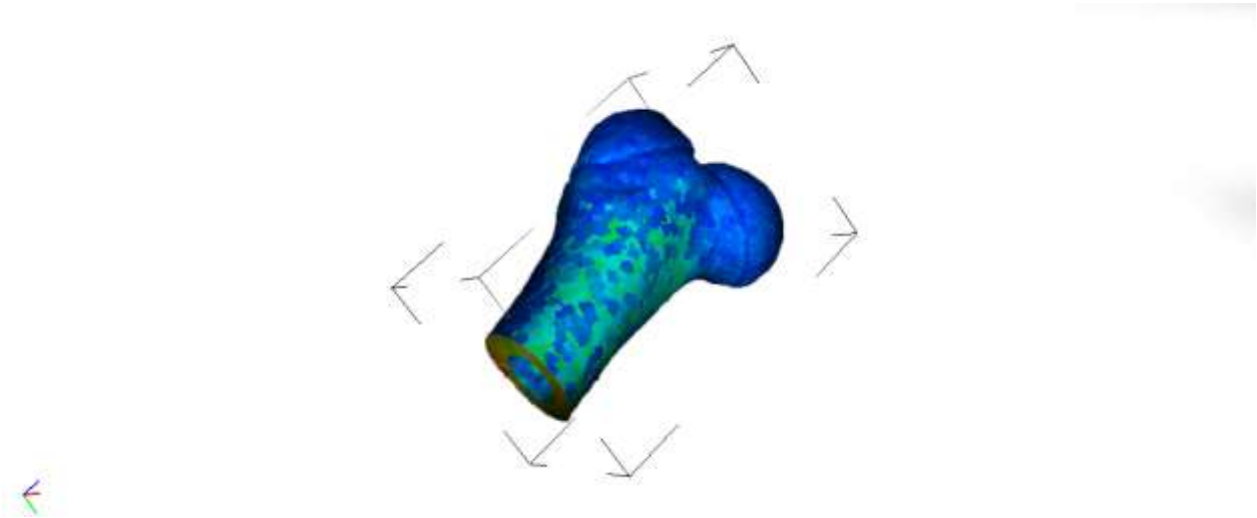

Fig. 6. Calculated values of output colour data, estimation of material properties by Bonemat LUT (Look Up Table) properties. Of a isotropic material assignment.

4. Results

The laboratory tests of the porcine femur were carried out, resulting in the graphs (figure 7), where the behaviour of a trabecular and cortical bone can be observed. This is because the femur is composed of high rigidity zones (intermediate section) and low rigidity zones (left and right sections).

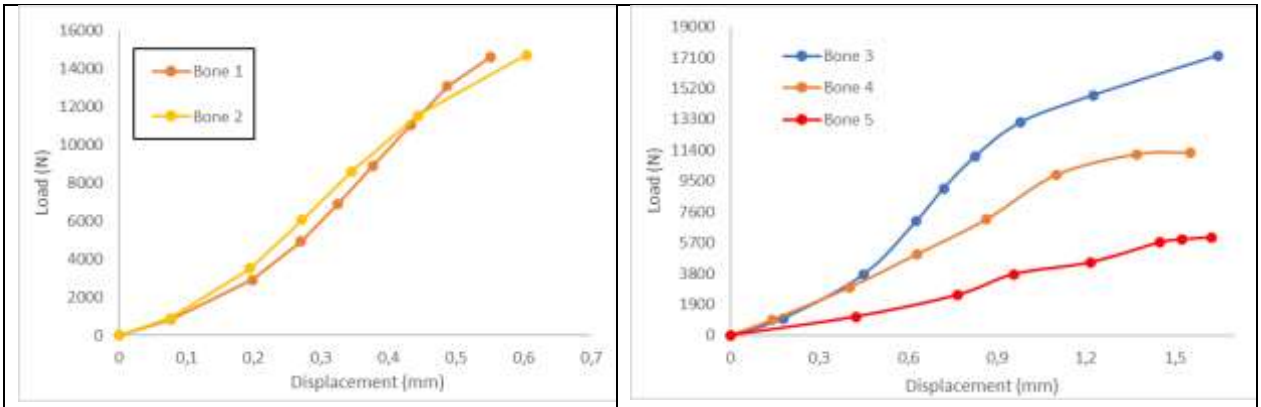

(a) (b)

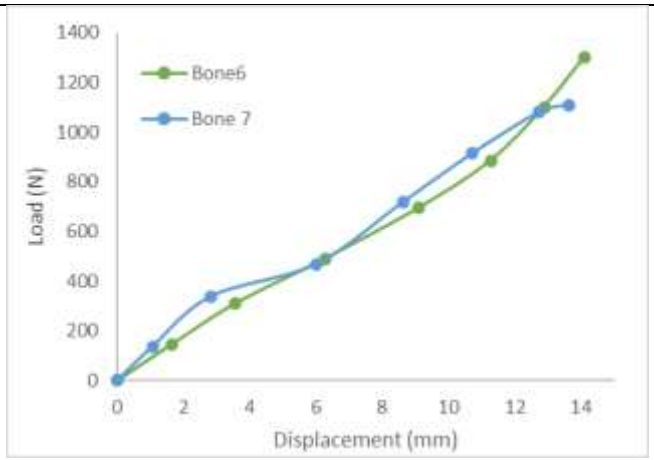

(c)

Fig. 7. stress-strain graph (a) cortical bone test, (b) cortical and trabecular bone test, (c) trabecular bone test

The results in greater detail can be seen in Table 4, Table 5 and Table 6, where the average load and deformation are observed. Table four shows a value with a higher load compared to table five and six, this is due to the fact that in that section of the bone to be analysed it is cortical, in other words, it is a more compact material in its formation, leaving spaces or gaps between each fiber closer together.

Table 4. Test results in MTS machine bone 1 and bone 2

Femur	Bone 1	Bone 2	Avarege (mm)	Avarege (N)
Displacement (mm)	0,551	0,604	0,578	16582,404
Load (N)	14614,138	18550,671		

The interaction of the bone section is reflected, which is compact due to the minimum deformation that is 0.578 mm.

Table 5. Test results in MTS machine bone 3, bone 4 and bone 5

Femur	Bone 3	Bone 4	Bone 5	Avarege (mm)	Avarege (N)
Displacement (mm)	1,645	1,553	1,622	1,587	11502,980
Load (N)	17218,727	11261,997	6028,215		

The behaviour of table 5 shows the values of two bone materials, cortical and trabecular, showing more compact sections and others with a greater space between them, where it gives us as a result 11.5 KN as a load to support and 1,587 mm of deformation, both average values.

Table 6. Test results in MTS machine bone 6 and bone 7

Femur	Bone 6	Bone 7	Avareg e (mm)	Avarege (N)
Displacement (mm)	15,789	13,642	14,716	1204,2
Load (N)	1300,689	1107,711		

The conduct of table 6 shows two sections of the bone that present a trabecular behavior, where it is possible to see their point of failure at a lower value of load than the other sections of the bones, which is 1,204 KN and a deformation of 14,716 mm, this is due to not being a compact bone in that section.

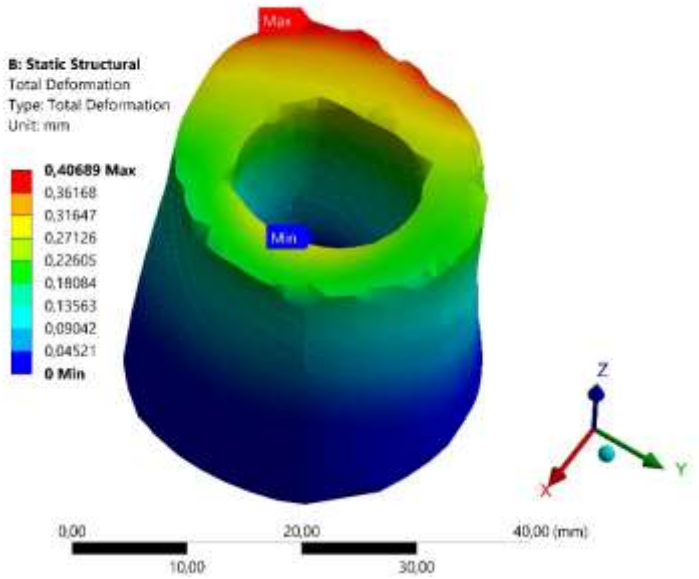

Fig. 8. Physical model of section 1 of the porcine femur, stress strain

The models that were subjected to laboratory tests, based on characterization, the numerical model was made, to replicate and establish an adequate method, based on the properties of the composite material (young's modulus), in figure 8 its maximum displacement 0,40 mm, this model was recreated with the same conditions of the laboratory tests.

5. Conclusions

The characterization of the porcine femur was carried out, giving as results, cortical and trabecular values in the sections that had been established. These parameters were taken into account for the development of the finite element model.
It is verified that the CAD models of the porcine bones were built based on the DICOM files obtained in the computerized axial tomography.
It is possible to conclude that the characterization of the physical models based on finite elements and with the information of the parameters of the laboratory test was carried out. Providing a suitable numerical methodology to recreate laboratory models.

6. References

[1] M. Ruess, D. Tal, N. Trabelsi, Z. Yosibash, and E. Rank, "The finite cell method for bone simulations: Verification and validation," *Biomech. Model. Mechanobiol.*, vol. 11, no. 3–4, pp. 425–437, 2012, doi:10.1007/s10237-011-0322-2.

[2] T. Dahmen, M. Roland, T. Tjardes, B. Bouillon, P. Slusallek, and S. Diebels, "An automated workflow for the biomechanical simulation of a tibia with implant using computed tomography and the finite element method," *Comput. Math. with Appl.*, vol. 70, no. 5, pp. 903–916, 2015, doi:10.1016/j.camwa.2015.06.009.

[3] W. Chen, N. Dai, J. Wang, H. Liu, D. Li, and L. Liu, "Personalized design of functional gradient bone tissue engineering scaffold," *J. Biomech. Eng.*, vol. 141, no. 11, 2019, doi:10.1115/1.4043559.

[4] "21st Polish Conference on Biocybernetics and Biomedical Engineering, PCBBE 2019," *Adv. Intell. Syst. Comput.*, vol. 1033, 2020.

[5] H. Naghibi *et al.*, "A noninvasive MRI based approach to estimate the mechanical properties of human knee ligaments," *J. Mech. Behav. Biomed. Mater.*, vol. 93, pp. 43–51, 2019, doi:10.1016/j.jmbbm.2019.01.022.

[6] P. Zellmann, I. Ribitsch, S. Handschuh, and C. Peham, "Finite element modelling simulated meniscus translocation and deformation during locomotion of the equine stifle," *Animals*, vol. 9, no. 8, 2019, doi:10.3390/ani9080502.

[7] L. Puggelli, F. Uccheddu, Y. Volpe, R. Furferi, and D. Di Feo, "Accuracy assessment of CT-based 3D bone surface reconstruction," *Lect. Notes Mech. Eng.*, pp. 487–496, 2019, doi:10.1007/978-3-030-12346-8_47.

[8] T. Damm, J. A. Peña, G. M. Campbell, J. Bastgen, R. Barkmann, and C.-C. Glüer, "Improved accuracy in the assessment of vertebral cortical thickness by quantitative computed tomography using the Iterative Convolution OptimizatioN (ICON) method," *Bone*, vol. 120, pp. 194–203, 2019, doi:10.1016/j.bone.2018.08.024.

[9] M. T. Bahia, E. G. F. Mercuri, and M. B. Hecke, "FE bone structural analysis with CT mapping of inhomogeneous material properties," in *ECCOMAS Congress 2016 - Proceedings of the 7th European Congress on Computational Methods in Applied Sciences and Engineering*, 2016, vol. 4, pp. 6574–6587.

[10] V. Baca, Z. Horak, P. Mikulenka, and V. Dzupa, "Comparison of an inhomogeneous orthotropic and isotropic material models used for FE analyses," *Med. Eng. Phys.*, vol. 30, no. 7, pp. 924–930, 2008, doi:https://doi.org/10.1016/j.medengphy.2007.12.009.

[11] Z. Zhu *et al.*, "Automated Segmentation of Swine Skulls for Finite Element Model Creation

Using High Resolution μ -CT Images," *Int. J. Comput. Methods*, vol. 16, no. 3, 2019, doi:10.1142/S0219876218420124.

[12] J. Y. Rho, M. C. Hobatho, and R. B. Ashman, "Relations of mechanical properties to density and CT numbers in human bone," *Med. Eng. Phys.*, vol. 17, no. 5, pp. 347–355, 1995, doi:https://doi.org/10.1016/1350-4533(95)97314-F.

[13] J. Moosmann *et al.*, "A load frame for in situ tomography at PETRA III," in *Proceedings of SPIE - The International Society for Optical Engineering*, 2019, vol. 11113.

[14] M. Mirkhalaf, A. Sunesara, B. Ashrafi, and F. Barthelat, "Toughness by segmentation: Fabrication, testing and micromechanics of architectured ceramic panels for impact applications," *Int. J. Solids Struct.*, vol. 158, pp. 52–65, 2019, doi:10.1016/j.ijsolstr.2018.08.025.

[15] Z. Li, J. Wang, G. Song, C. Ji, and X. Han, "Anisotropic and strain rate-dependent mechanical properties and constitutive modeling of the cancellous bone from piglet cervical vertebrae," *Comput. Methods Programs Biomed.*, vol. 188, 2020, doi:10.1016/j.cmpb.2019.105279.

[16] G. Szebényi, P. Görög, A. Török, and R. M. Kiss, "Effect of different conservation methods on some mechanical properties of swine bone," in *WIT Transactions on Biomedicine and Health*, 2013, vol. 17, pp. 225–233.

[17] T. M. Keaveny, T. P. Pinilla, R. P. Crawford, D. L. Kopperdahl, and A. Lou, "Systematic and random errors in compression testing of trabecular bone," *J. Orthop. Res.*, vol. 15, no. 1, pp. 101–110, Jan. 1997, doi:10.1002/jor.1100150115.

[18] E. Schileo *et al.*, "An accurate estimation of bone density improves the accuracy of subject-specific finite element models," *J. Biomech.*, vol. 41, no. 11, pp. 2483–2491, 2008, doi:https://doi.org/10.1016/j.jbiomech.2008.05.017.

[19] W. A. Kalender, "A phantom for standarization and quality control in spinal bone mineral measurements by QCT and DXA: Design considerations and specifications," *Med. Phys.*, vol. 19, no. 3, pp. 583–586, May 1992, doi:10.1118/1.596899.